energies

MDPI

Article

Energy Recovery from Municipal Sewage Sludge: Combustion Kinetics in a Varied Oxygen–Carbon Dioxide Atmosphere

Jurand Bień * and Beata Bień

Faculty of Infrastructure and Environment, Czestochowa University of Technology, 42-200 Czestochowa, Poland; beata.bien@pcz.pl

* Correspondence: jurand.bien@pcz.pl

Abstract: Energy from municipal sewage sludge can be obtained by applying a thermal conversion method. In this study, the combustion kinetics of municipal sewage sludge were analyzed in an O_2/CO_2 atmosphere. Studies were conducted in different gaseous atmospheres consisting of varying proportions of oxygen and carbon dioxide. The participation of oxygen was as follows: 20, 40, 60, 80 and 100% vol. The experimental temperatures varied from 873 to 1273 K. The experimentally obtained results helped establish the basic kinetic parameters, such as the reaction order n, factor Ko and activation energy E_a of sludge grains. The values of the activation energy E_a and K_o were, respectively, 46 kJ/mol and 0.0127 mg/m^{2}sPa. They show that the limiting factor of combustion is the diffusion of oxygen and that combustion reactions take place in the outer layer of the unreacted core. Therefore, sludge is promising for energy recovery because it has quite a high net calorific value (NCV) and a high gross calorific value (GCV). The GCV was 14.1 MJ/kg and the NCV was 12.8 MJ/kg. The experimental studies with a wide range of process parameters helped to create an array of apparent reaction rates as a function of the temperature and oxygen concentration, showing the significant effect of oxygen on the apparent reaction rate, in contrast to the effect of temperature.

Keywords: sewage sludge; O_2/CO_2 atmosphere; energy activation; apparent reaction rate; thermogravimetry

check for updates

Citation: Bień, J.; Bień, B. Energy Recovery from Municipal Sewage Sludge: Combustion Kinetics in a Varied Oxygen–Carbon Dioxide Atmosphere. *Energies* **2024**, *17*, 5382. https://doi.org/10.3390/en17215382

Academic Editor: Constantinos Noutsopoulos

Received: 26 September 2024
Revised: 14 October 2024
Accepted: 25 October 2024
Published: 29 October 2024

Copyright: © 2024 by the authors. Licensee MDPI, Basel, Switzerland. This article is an open access article distributed under the terms and conditions of the Creative Commons Attribution (CC BY) license (https://creativecommons.org/licenses/by/4.0/).

1. Introduction

Municipal sewage sludge is a by-product of wastewater treatment and is not a typical fuel; however, it has some energy. The chemical composition of sewage sludge is not constant but variable, depending closely on the type of wastewater being treated, the method of treatment, and the processing procedures at the treatment plant [1–4]. Usually, sewage sludge is characterized by a high moisture content, with a value of about 80% after mechanical dewatering, a high mineral fraction content, which can constitute around 50% of the sludge's dry mass and a high content of volatile compounds, which can be as much as 90% in a dry, ash-free state. These parameters mean that the combustion mechanism of sewage sludge granules can differ significantly from the combustion mechanism of coal particles or wastes [5,6]. While both combustion and gasification share certain kinetic mechanisms—especially up to the point where CO is oxidized to CO_2—combustion in an O_2/CO_2 atmosphere involves higher oxidation levels and focuses on the oxidation of carbon compounds. Gasification, on the other hand, typically produces syngas (CO, H_2), which is not the case in full combustion. In the combustion process, a sequence of processes can be distinguished, such as drying, devolatilization, and combustion of volatile matter, followed by combustion of the coke fraction, which in the case of sewage sludge contains significant amounts of mineral compounds. The devolatilization process for sludge begins at a relatively low temperature (100 °C), which makes its behavior similar to that of lignite [7,8]. Furthermore, sewage sludge devolatilization starts upon complete drying, whereas this process in coal partially overlaps with drying. Well-known studies

by Werther et al. [9] have shown that the devolatilization time for wet sludge granules ranging from 4 to 20 mm in size was 100–300 s, whereas for partially dried sludge of the same granule size it was 50 s. The devolatilization and combustion of volatile matter in the case of sludge is a critical element of the combustion process. The time required to burn the coke residue in sewage sludge is much longer than the time needed to burn the volatile matter. This is partly due to the low elemental carbon content in the coke residue. The reactivity of the coke residue can be understood by studying its kinetics. The combustion of elemental carbon, in its simplest form, is its high temperature oxidation to carbon dioxide according to Equation (1):

$$C + O_2 \rightarrow CO_2 + 394\ kJ/mol \quad (1)$$

Oxygen diffuses to the surface of the coke granule, leading to oxidation into carbon monoxide, which subsequently oxidizes to carbon dioxide in the gas phase near the coke granule's surface. The carbon dioxide formed is the primary combustion product. This mechanism is dominant at low Reynolds numbers for coke granules with diameters greater than 1 mm and at high temperatures in the range of 900–1300 °C, as shown by the study of Ross et al. [10]. However, this is not the only mechanism to be considered in coke granule combustion. Studies by Basu et al. [11] have shown that oxygen diffusion toward the surface of the coke granule leads to the formation of both carbon monoxide and carbon dioxide. Carbon monoxide in the gas phase reacts with oxygen, resulting in the formation of carbon dioxide. The chemical reactions proceed according to the following equations:

$$C + ½O_2 \rightarrow CO + 111\ kJ/mol \quad (2)$$

$$C + O_2 \rightarrow CO_2 + 394\ kJ/mol \quad (3)$$

$$CO + ½O_2 \rightarrow CO_2 \quad (4)$$

Taking the above into account, Rajan et al. [12], by introducing the coefficient ϕ, developed an equation describing the mechanism of carbon monoxide and carbon dioxide formation as a result of coke residue oxidation:

$$C + 1/\phi\ O_2 \rightarrow (2 - 2/\phi)CO + (2/\phi - 1)CO_2 \quad (5)$$

Determining the combustion kinetics parameters based on the loss of organic matter must consider the appropriate combustion model, which takes into account the correct combustion mechanism depending on the conditions in the combustion zone. The literature distinguishes different combustion models, including the Shrinking-Particle Model (SPM), the Shrinking-Core Model (SCM), and the Shrinking-Density Model (SDM) [13–15].

Numerous studies have investigated the kinetics of sewage sludge thermochemical valorization processes such as pyrolysis and gasification [16–21]. However, the kinetics of sewage sludge incineration have received limited attention. Liu et al. [22], for example, performed kinetic analysis of a pure sewage sludge using two isoconversional methods, Flynn–Wall–Ozawa (FWO) and Kissinger–Akahira–Sunose (KAS), under oxy-fuel and air environments, while Aidabulow et al. [23] used thermogravimetric analysis to explore combustion kinetics, providing updated data on the emission patterns during the co-combustion of sewage sludge with high-ash bituminous coal. Hernandez et al. investigated the incineration of sewage sludge under different atmospheres (N_2, CO_2 and air) using TGA-FTIR in order to understand the effects of different atmospheric gases on the kinetics of degradation and on the gaseous products [24]. He noticed that the higher oxidative degree of the atmosphere surrounding the sample resulted in higher reaction rates and a shift in the degradation mechanisms to lower temperatures, especially for the mechanisms taking place at temperatures above 673 K. In conclusion, Hernandez et al. stated that the kinetics for different processes require a different approach for their scaling up and specific consideration of their characteristic reaction temperatures and rates should be evaluated [24]. This inspired us to perform experiments on the combustion of municipal digested sewage sludge in five different gaseous atmospheres consisting of varying propor-

tions of oxygen and carbon dioxide. The participation of oxygen in the gaseous mixture was 20, 40, 60, 80 and 100% vol and the combustion temperatures were within 873–1273 K. The novelty of this research lies in its detailed examination of how the oxygen concentration and particle size affect the combustion process. Our study highlights the critical role of oxygen diffusion in determining the apparent reaction rate, an aspect not sufficiently covered in gasification studies. The experiments were designed to provide detailed kinetic data, including the reaction orders, activation energy, and pre-exponential factors, which can optimize sludge combustion processes, particularly in waste-to-energy applications. Unlike studies on gasification, where partial oxidation leads to syngas production, this study focuses on the full oxidation pathway, offering new insights that can be applied in combustion systems.

2. Materials and Methods

The research material was digested sewage sludge. The sludge was collected from a wastewater treatment plant located in a large urban–industrial agglomeration in Poland. The primary sludge, after thickening, is directed to an anaerobic digestion chamber where it undergoes the typical stages of digestion: hydrolysis, acidogenesis, acetogenesis, and methanogenesis. For this study, the digested sludge was collected after the completion of the methanogenesis stage, when most of the organic matter had been converted into biogas, and the sludge was ready for subsequent dewatering and drying. The physical and chemical properties of the sewage sludge reported in Table 1 were determined using standardized testing procedures. The following Polish Standards (PN) and documented analytical methods were applied: sample preparation (PN-G-04502:2014-11), which outlines the basic methods for sampling and preparation for laboratory analysis, moisture content (PN-ISO 1015:1998), ash content (PN-ISO 1171:2002P), volatile matter (PN-G-04516:1998), and calorific value (PN-ISO 1928:2002P). Moreover, the elemental composition of carbon, hydrogen and nitrogen was measured using automatic analyzers, following PN-G-04571:1998 and the sulfur content was analyzed using automatic analyzers in compliance with PN-G-04584:2001.

Table 1. Technical and elemental analysis of the studied municipal sewage sludge.

Technical Analysis		Elemental Analysis	
Gross calorific value	14,095 kJ/kg	Carbon (C)	34.83%
Net calorific value	12,848 kJ/kg	Sulphur (S)	1.36%
Moisture (W)	6.65%	Hydrogen (H)	4.99%
Ash (A)	35.35%	Nitrogen (N)	3.44%
Volatile matter (V)	49.35%	Oxygen (O) (by difference)	13.38%
Coke (by difference)	8.65%		

X-ray fluorescence (XRF) analysis of both the sewage sludge and the ash after incineration was also conducted. The results are presented in Table 2. In the sewage sludge, iron compounds dominate, with nearly 38% of the composition. Significant contributions are also observed from CaO, SO_3, P_2O_5, and SiO_2 compounds. In the ash, Fe_2O_3, CaO, SiO_2, and P_2O_5 are present in the largest quantities.

To determine the kinetic parameters of sewage sludge combustion in a variable O_2/CO_2 atmosphere, the thermogravimetric method was employed. The tests were conducted as dynamic (non-isothermal) and static (quasi-isothermal) tests on sieved sewage sludge particles with a diameter of 1000 and 2000 μm. The sample mass for each test was 10 ± 1 mg. The experiments were performed using a TGA/SDTA 851e thermogravimetric analyzer from Mettler-Toledo, Warsaw, Poland which simultaneously recorded the sample weight loss and the sample temperature under the strictly controlled conditions of the modified atmosphere applied. Five different gas atmospheres were used based on different oxygen and carbon dioxide volume proportions. The oxygen content was set to 20%, 40%, 60%, 80%, and 100% by volume, respectively. The tests were conducted at the following

temperature points: 873 K, 973 K, 1073 K, 1173 K, and 1273 K. Heating to the target temperature was carried out in a nitrogen atmosphere at a heating rate of 50 K/min, after which the system was switched to the appropriate reactive O_2/CO_2 atmosphere (Figure 1). The flow rate of the reactive gas through the measurement cell was maintained at a constant level of 50 mL/min. During the non-isothermal testing, the sample in the modified atmosphere was heated to 1273 K, with constant heating rates of 10, 20, 30 and 40 K/min, in an open crucible. Before each test, blank runs with empty crucibles were conducted to compensate for buoyancy.

Table 2. Results of the XRF analysis of municipal sewage sludge and ash from sludge combustion.

Sewage Sludge		**Ash**	
Al_2O_3	4%	Al_2O_3	6.1%
SiO_2	10%	SiO_2	17%
P_2O_5	14%	P_2O_5	17.2%
SO_3	9.41%	SO_3	3%
K_2O	0.66%	K_2O	0.75%
CaO	19.2%	CaO	20.4%
TiO_2	1.2%	TiO_2	1.12%
V_2O_5	0.04%	V_2O_5	0.04%
Cr_2O_3	0.25%	Cr_2O_3	0.23%
MnO	0.17%	MnO	0.16%
Fe_2O_3	37.79%	Fe_2O_3	32.36%
NiO	0.12%	NiO	0.089%
CuO	0.23%	CuO	0.16%
ZnO	1.52%	ZnO	1.12%
SrO	0.092%	Rb_2O	0.01%
ZrO_2	0.063%	SrO	0.062%
RuO_2	0.92%	ZrO_2	0.044%
BaO	0.2%	BaO	0.24%
Eu_2O_3	0.23%	HgO	0.02%

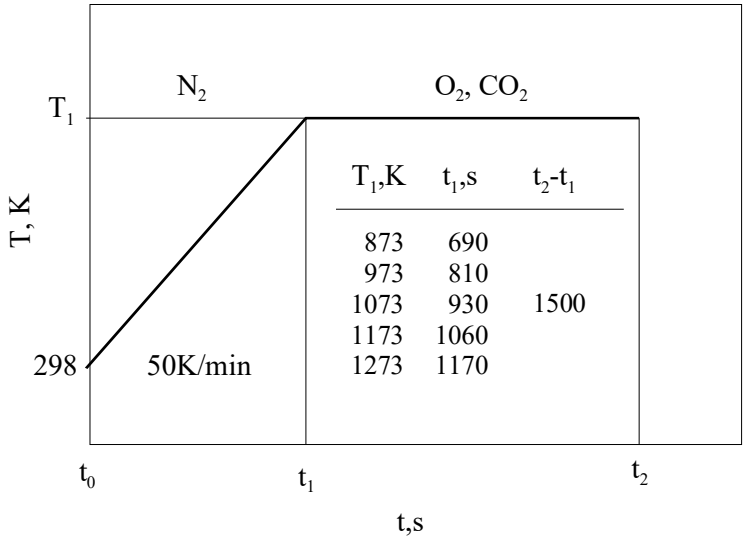


Figure 1. Quasi-isothermal test scheme to study sludge combustion kinetics.

The recorded data were exported as a text file from the STARe Mettler-Toledo software and imported into Excel for further processing.

The reaction rate of the degradation of a material is expressed as a derivative of the rate of conversion of the substance over time ($d\alpha/dt$). This rate is a linear function of

the temperature-dependent reaction rate constant $k(T)$ and the temperature-independent conversion function $f(\alpha)$:

$$\frac{d\alpha}{dt} = k(T)f(\alpha) \tag{6}$$

where α is the conversion constant, t is the time, T is the absolute temperature and $k(T)$ is described by the Arrhenius equation:

$$k(T) = Aexp\left(-\frac{E_A}{RT}\right) \tag{7}$$

where k represents the reaction rate constant, E is the activation energy, A is the preexponential factor, T is absolute temperature and R is the universal gas constant [25]. A number of kinetic models defining the form of the function $f(\alpha)$ have been developed on the basis of studies of the geometry of reaction surfaces [26]. Some of them are presented in Table 3.

Table 3. Some of the conversion functions $f(\alpha)$ [26].

Symbol	Function Form f(α)	Reaction Model
A2	$2(1-\alpha)[-\ln(1-\alpha)]^{1}/^{2}$	Two-dimensional nucleation growth, Avrami–Erofeev equation
A3	$3(1-\alpha)[-\ln(1-\alpha)]^{2}/^{3}$	Three-dimensional nucleation growth, Avrami–Erofeev equation
An* [1]	$n(1-\alpha)[-\ln(1-\alpha)]^{(n-1)/n}$	n-dimensional nucleation growth, Avrami–Erofeev equation
B1	$(1-\alpha)\alpha$	Autocatalytic reaction, Prout–Tompkins equation
F1	$(1-\alpha)$	First-order reaction
F2	$(1-\alpha)^{2}$	Second-order reaction
Fn* [1]	$(1-\alpha)^{n}$	n-th order reaction
R2	$2(1-\alpha)^{1}/^{2}$	Two-dimensional phase boundary movement reaction
R3	$3(1-\alpha)^{2}/^{3}$	Three-dimensional phase boundary movement reaction
D1	$1/2\alpha$	One-dimensional diffusion
D2	$1/[-\ln(1-\alpha)]$	Two-dimensional diffusion
D3	$3(1-\alpha)^{2}/^{3}/2[1-(1-\alpha)^{1}/^{3}]$	Three-dimensional diffusion, Jander's equation
D4	$3/2[(1-\alpha)^{-1}/^{3}-1]$	Three-dimensional diffusion, Ginstling–Brounshtein equation

[1] n*—reaction rate.

In such an approach, we try fitting to the nature of the conversion function, but in the iso-conversion methodology, the kinetic parameters can be determined without the problem of identifying the correct kinetic model. The combination of Equations (6) and (7) leads to:

$$\frac{d\alpha}{dt} = Aexp\left(-\frac{E_A}{RT}\right)f(\alpha) \tag{8}$$

where, for non-isothermal tests conducted with a linear heating factor $\beta = dT/dt$, Equation (8) can be transformed to:

$$\frac{d\alpha}{f(\alpha)} = \frac{A}{\beta}exp\left(-\frac{E_A}{RT}\right)dT \tag{9}$$

As all the experiments are conducted at constant partial pressures of oxygen, a function $g(\alpha)$ can be defined based on integrating Equation (9).

$$g(\alpha) = \int_0^{\alpha}\frac{d\alpha}{f(\alpha)} = \frac{A}{\beta}\int_{T_0}^{T}exp\left(-\frac{E_A}{RT}\right)dT \tag{10}$$

where $T = T_0 + \beta t$, and T_0 is a starting temperature. For the determination of the apparent rate of the combustion reaction, Equation (7) can be represented as:

$$r_c(T, P_{O_2}) = \frac{dm}{d\tau} = Aexp\left(-\frac{E_A}{RT}\right)f(\alpha) = \frac{K_0}{F_e}P_{O_2}^{n}f(\alpha) \tag{11}$$

where F_e is the reaction surface area, $dm/d\tau$ is the organic mass loss, P_{O2} is the partial pressure of oxygen and K is the reaction rate. For thermogravimetric studies, the apparent

reaction rate, defined in [g/m^{2}s], can be determined directly from the TG curves, but a prerequisite for its determination is still the knowledge of the current reaction surface F_e. This value can be estimated as:

$$F_{ei} = \pi d_{ci}^2 n_s \tag{12}$$

where n_s is a number of fuel grains. The diameter of d_{ci} is determined as follows:

$$d_{ci} = \left(\frac{m_i - m_p}{\rho_{cm} {}^1/_6 \pi n_s} \right)^{1/3} \tag{13}$$

where m_p is the mass of ash and the density of the organic matter of the fuel (ρ_{cm}) is determined from the following equation.

$$\rho_{cm} = \left(\frac{m_1 - m_p}{{}^1/_6 \pi d_{c1}^3 n_s} \right) \tag{14}$$

In the following, the conversion rate of the fuel organic matter (X) was determined from relation (15), where m_1 is the initial mass of the fuel, m_i is the mass of the fuel in the next calculation step and m_p is the mass of the ash.

$$X = 1 - \frac{m_i - m_p}{m_1 - m_p} \tag{15}$$

3. Results and Discussion

3.1. Effect of Sludge Grain Size on the Apparent Rate of the Combustion Reaction

To assess the fuel particle size, sewage sludge of two different sizes was tested. In the first case, particles with a diameter of 1.0×10^{-3} m were used. In the second, particles twice as large were used. The relationship between the reaction rate and the partial pressure of oxygen at a temperature of 1073 K for particles with diameters of 1000 µm (1 mm) and 2000 µm (2 mm) is presented in Figures 2 and 3, respectively.

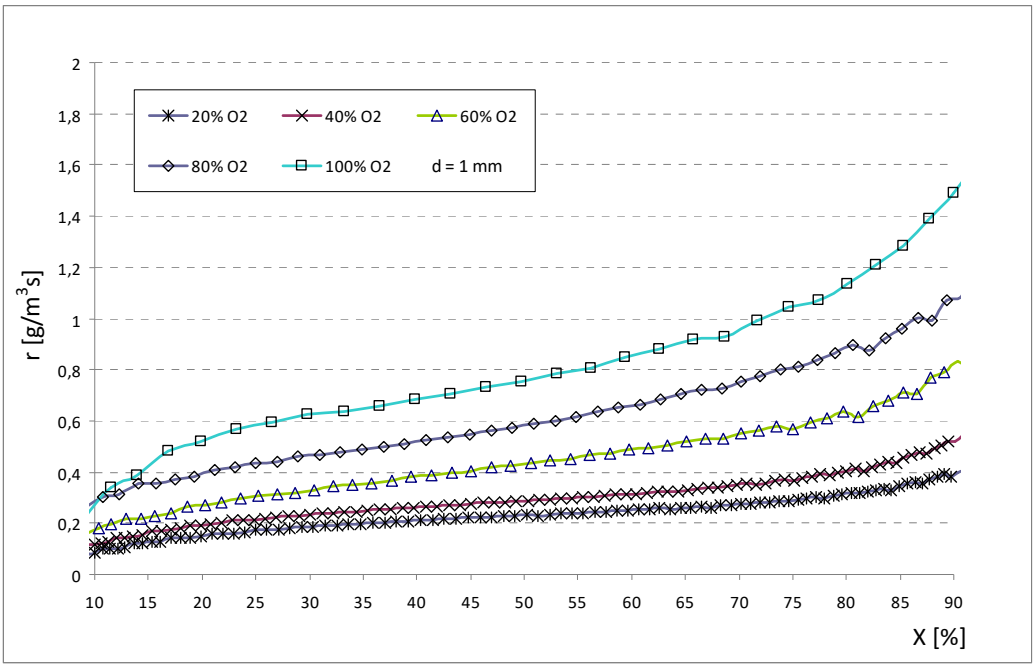


Figure 2. The apparent reaction rate of combustion as a function of the fuel conversion rate (d = 1 mm).

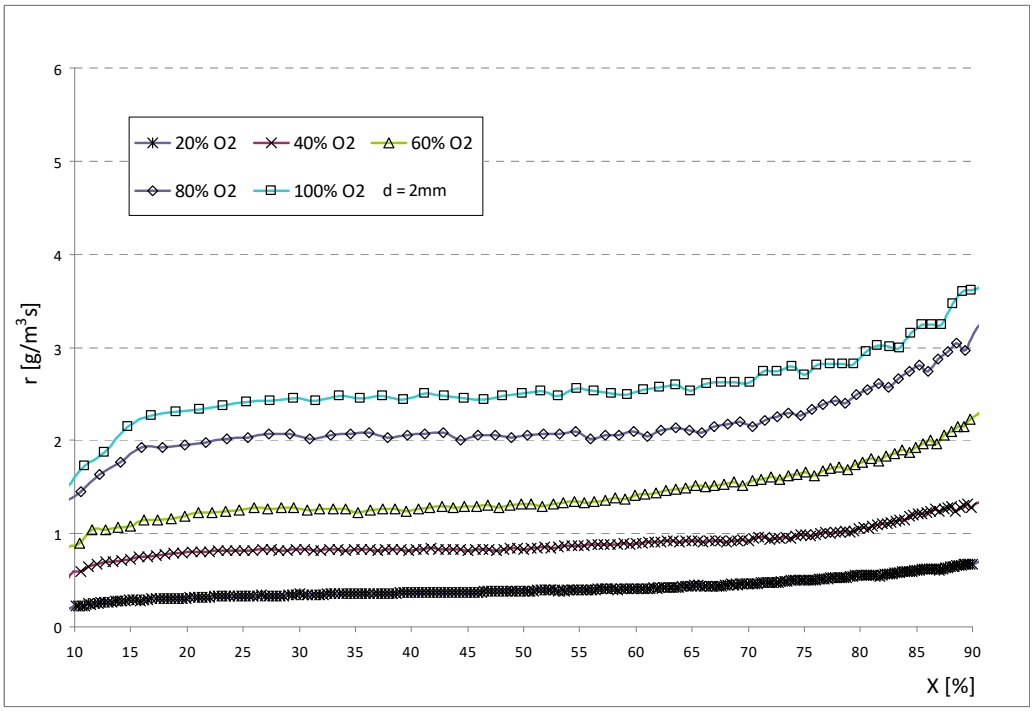


Figure 3. The apparent reaction rate of combustion as a function of the fuel conversion rate (d = 2 mm).

The data indicate that as the partial pressure of oxygen increases, the reaction rate significantly rises. This increase is much more noticeable for particles with a diameter of 2 mm. Of particular interest is the behavior of the fuel particle temperature relative to the temperature of the reactive gas with an increasing oxygen concentration. It can be observed that as the oxygen concentration increases, there is an increase in the surface temperature of the fuel particle relative to that of the reaction gas. Although this is the expected reaction, it is important because the exact values of these parameters, as determined for different thermal conditions at different partial pressures of oxygen in the gaseous atmosphere, are necessary for the precise determination of the reaction kinetic parameters, such as the reaction order n, the pre-exponential coefficient K_o or the activation energy E_a [27]. Determination of the kinetic parameters of sludge combustion in a modified O_2/CO_2 atmosphere was carried out using the mean values of the apparent reaction rate r, which were determined for a fuel conversion rate in the range X = 40–60%, taking into account the logarithmic form of Equation (11). From the experimental data, we extracted the combustion rate (r), oxygen partial pressure (PO_2), and conversion (α) to compute the apparent reaction rate. Both the reactive gas temperature and the fuel particle surface temperature were measured. Due to the excessive differences between the fuel particle temperature and the reactive gas temperature ΔT, as shown in Figure 4, the apparent reaction rate values for the process conducted at the 80% and 100% oxygen concentrations were excluded from the calculations. Under conditions of lower partial pressures, the fuel particle temperature rise remained within 1%.

Based on the plotted dependence of the apparent reaction rate on the partial pressure of oxygen (Figure 5), the apparent reaction order was determined for the sludge tested. For sludge with a diameter of 1 mm, the reaction order was n = 0.82, and for sludge with a grain size of 2 mm, the reaction order was n = 0.86. These values are in line with those found in the literature [28,29].

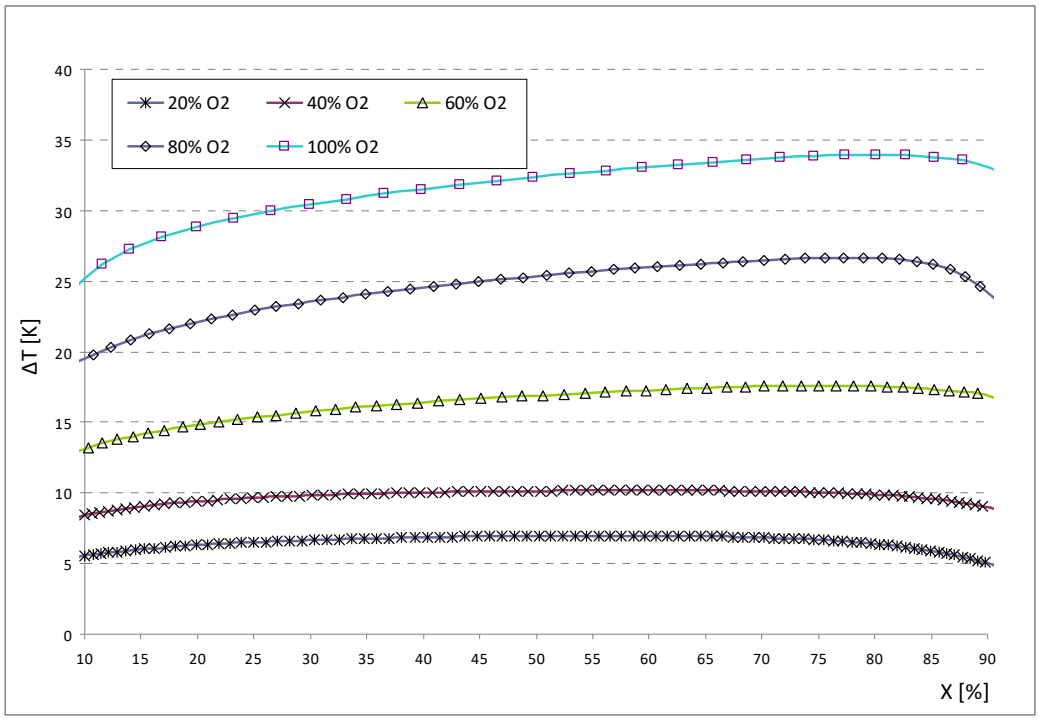


Figure 4. The increase in the fuel sample temperature in relation to the gas reaction temperature as a function of the fuel conversion rate.

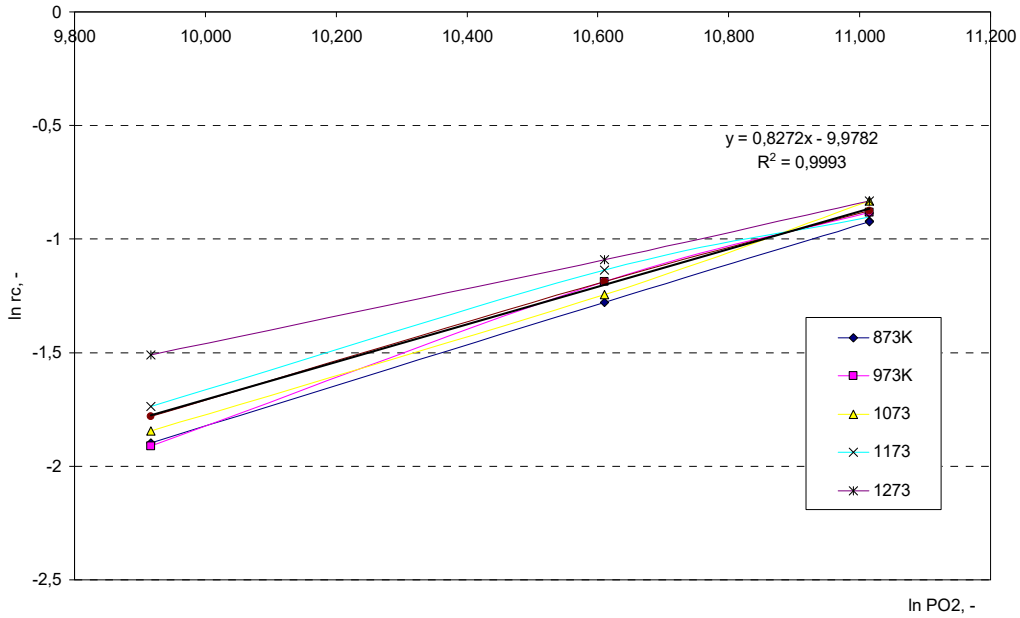


Figure 5. Diagram of the dependence of the apparent reaction rate on the partial pressure of oxygen of the sludge combustion reaction.

Based on the Arrhenius equation indicating the inversely linear temperature dependence of the reaction rate constant and on experimental data (Figure 6), the activation energy E_a and the pre-exponential coefficient K_o were determined. In our study, two particle sizes were tested: 1.0 mm and 2.0 mm. For the smaller grains and the conversion rates in the range of 40–60%, the values of the activation energy E_a and K_o were, respectively, 45.57 kJ/mol (10.9 kcal/mol) and 0.0127 mg/m^{2}sPa. For grains with a diameter of d = 2000 µm, the determined values of E_a and K_o were as follows: 31.92 kJ/mol (7.66 kcal/mol) and 0.033 mg/m^{2}sPa. The activation energy for particles with a larger

grain size is lower than for particles with a smaller size and it depends on the mechanism governing the combustion process analyzed. Hu et al. [30], who investigated the oxidation kinetics of coal-char particles with diameters in the range of 1.0 mm to 1.2 mm, indicated that if the value of the activation energy is in the range E_a = 17–23 kcal/mol, then the mechanism responsible for combustion is an intrinsic-diffusion mechanism. In contrast, the activation energy in the range E_a = 35–45 kcal/mol corresponds to a kinetic mechanism. In our experiments, as mentioned above, we observed that the activation energies for smaller sludge particles (1 mm) were 45.57 kJ/mol, while for larger particles (2 mm), the activation energy was 31.92 kJ/mol. These results suggest that for the smaller particle size, the combustion is primarily governed by a kinetic mechanism, consistent with the findings of Hu et al., while for the larger particles, diffusion plays a more significant role in limiting the reaction rate, as lower activation energy is indicative of a diffusion-controlled mechanism. Experimental investigations over a wide range of process parameters (temperature in the range 873–1273 K and oxygen partial pressure in 20–100% vol) allowed the development of a table of the apparent reaction rate parameter r_c, as is given in Table 4.

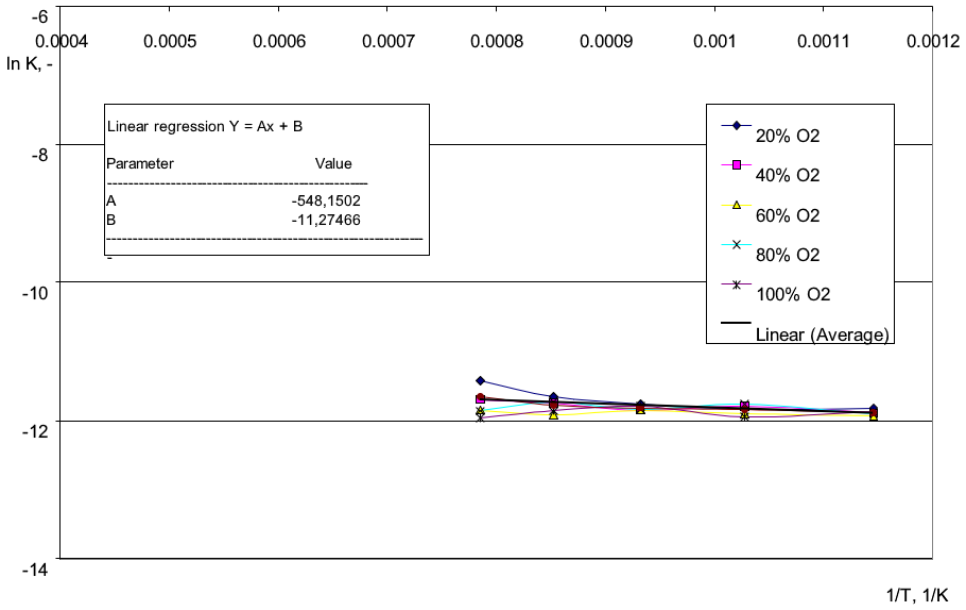


Figure 6. The reaction rate constant K as a function of the temperature.

Table 4. Apparent combustion reaction rate parameter of the tested sewage sludge as a function of the temperature and oxygen concentration.

$r_c(T,P_{O_2})=KP_{O_2}^n$	873 K	973 K	1073 K	1173 K	1273 K
20% O_2	0.137	0.147	0.154	0.161	0.167
40% O_2	0.275	0.293	0.309	0.323	0.335
60% O_2	0.412	0.440	0.463	0.484	0.502
80% O_2	0.549	0.586	0.618	0.645	0.669
100% O_2	0.687	0.733	0.772	0.806	0.837

As the temperature and reaction gas concentration increase, the apparent reaction rate increases. The oxygen concentration plays a much greater role in the process, as it determines the rate of the reaction, regardless of the thermal conditions. The effect of the temperature on the reaction rate is much smaller.

3.2. The Influence of the Heating Rate of Sewage Sludge Derived from TG Analyses

Investigations of the heating rate of the sludge (10, 20, 30 and 40 K/min) in a variable O_2/CO_2 atmosphere indicate that the thermogravimetric curves became increasingly close

as the heating rate increased. The percentage mass loss is 65.26% for a heating rate ratio of 10 K/min and increases slightly for a heating rate ratio of 40 K/min (65.97%). This behavior does harmonize with the thermogravimetric analysis (TGA) theory, where higher heating rates usually lead to faster thermal decomposition, causing a higher rate of volatile release and therefore greater mass loss over a shorter period. The first weight loss occurs in the temperature range 100–140 °C and is due to the evaporation of moisture (Figure 7). The second and third temperature ranges are 285–320 °C and 480–510 °C, respectively. As the heating rate coefficient increases, no shift in the temperature of the sample mass loss peak is observed. At a heating rate of 10 K/min, the greatest mass loss occurs at 308 °C, while at a rate of 40 K/min, the greatest mass loss peak occurs at 314 °C. There is an increase in the mass loss rate from 1.86% min^{-1} to 9.11% min^{-1} as the heating rate increases from a value of 10 K/min to 40 K/min. The increase in the oxygen concentration enhances the combustion efficiency, leading to more complete combustion even at lower temperatures. As a result, the mass loss becomes less dependent on the heating rate since the oxygen diffusion to the particle surface becomes the limiting factor.

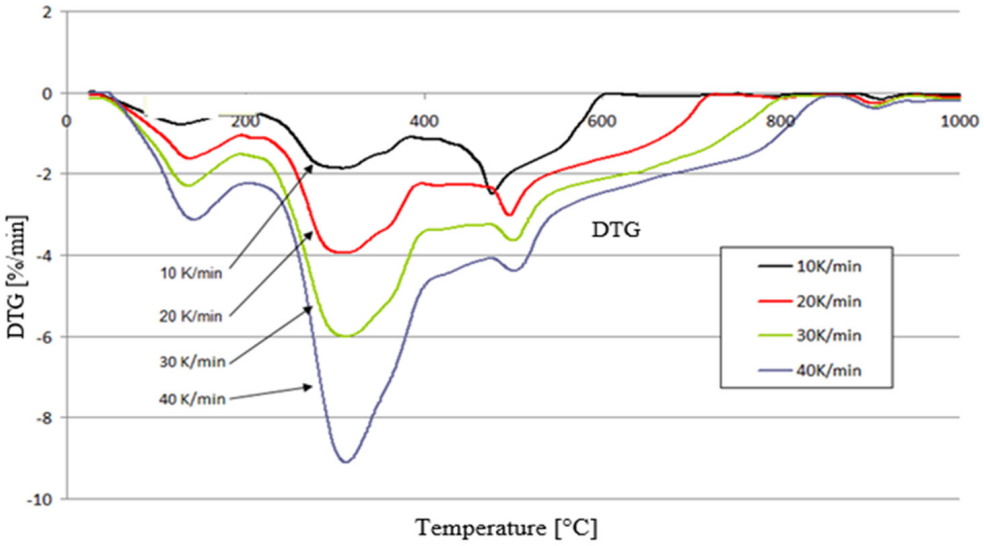


Figure 7. The rate of weight loss of sewage sludge as a function of the temperature at 20%O_2/80%CO_2 atmosphere.

3.3. The Weight Loss of Sewage Sludge in Modified Atmosphere Derived from TG Analyses

The TG curves at different oxygen volume fractions and at a heating rate of 20 K/min are shown in Figure 8. Analysis of the curves clearly shows that an increase in the oxygen concentration leads to a shift in the thermogravimetric curve to the left, i.e., into the lower temperature range. This shift is observed in the temperature range 200–600 °C. Below a temperature of 200 °C, the curves run very close to each other, even overlapping with one another. Then, it can be observed that while the oxygen concentration has a limited effect on the initial stages of thermal decomposition, as the oxygen concentration increases, particularly at levels of 80%, there is a significant increase in the mass loss and a noticeable shift in the thermal decomposition pattern. This suggests that the oxygen concentration plays an important role in enhancing the combustion process at higher levels. We observed the rapid release and combustion of volatile parts in a rather narrow temperature range between 230 and 270 °C. Significant mass loss takes place in the temperature range 200–600 °C, over 96%. Similar results were obtained with the combustion of algae [31] and lignite [32].

The difference thermogravimetry (DTG) curves of the mass loss rates of the test samples are given in Figure 9. Significant mass loss is observed from the release of volatile parts in the low temperature range 220–270 °C. The higher the oxygen concentration, the higher the rate of decomposition that occurs. The DTG curves also indicate a shift in the

sample mass loss profile into the lower temperature range as the oxygen concentration in the gas mixture increases. This is consistent with studies performed by Lai et al. [33].

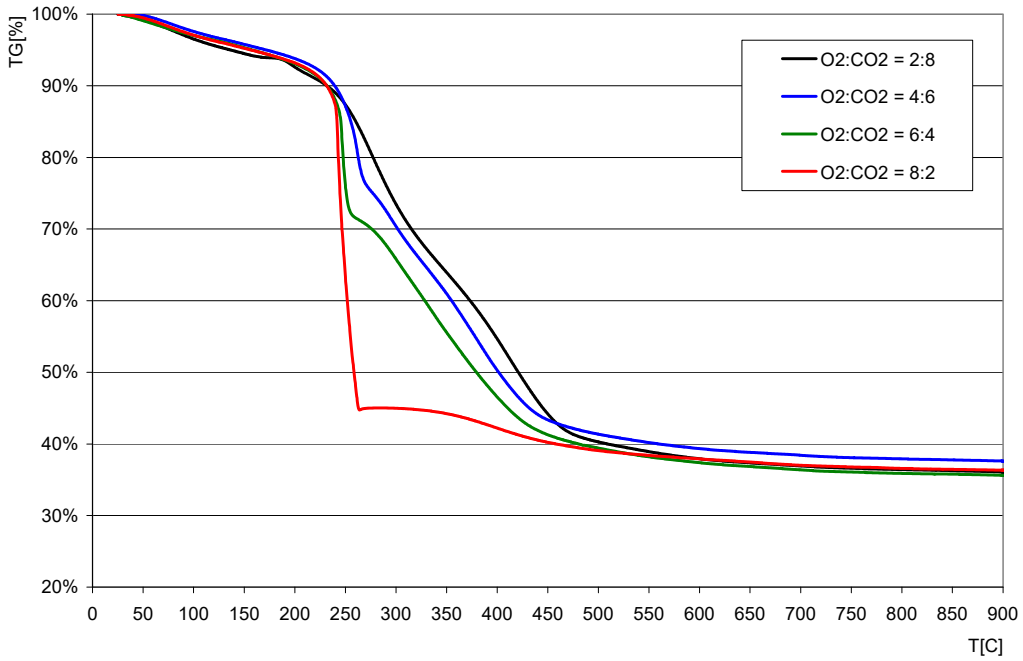


Figure 8. TG profiles at varying oxygen contents in an O_2/CO_2 mixture.

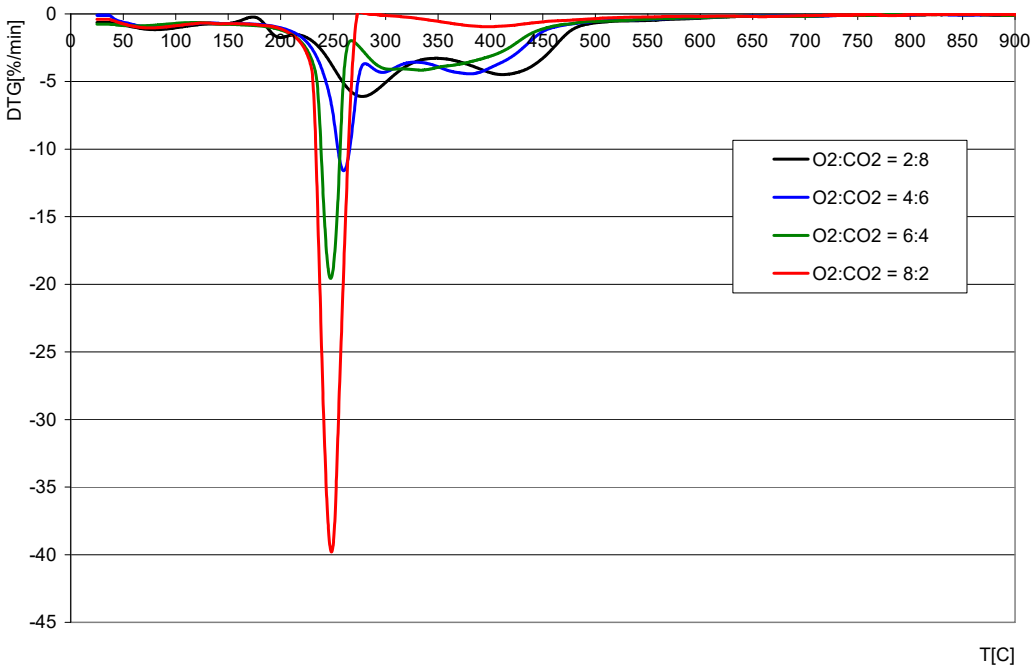


Figure 9. DTG profiles at varying oxygen contents in an O_2/CO_2.

The characteristic parameters of the thermal decomposition of the samples are summarized in Table 5.

The ignition temperature of sewage sludge occurs between 245 and 288 °C and decreases with an increasing oxygen concentration in the gas mixture. This is due to the increased mass flow of oxygen toward the surface of the particle. A similar phenomenon was observed by Yi et al. [34] during the combustion of coals in an O_2/CO_2 atmosphere.

Table 5. Characteristic parameters of sludge combustion profiles in a modified atmosphere.

[°C/min]	T1 [1] [°C]	D1 [% min^{-1}]	T2 [°C]	D2 [% min^{-1}]	T3 [°C]	D3 [% min^{-1}]	Tmax [°C]	Dmax [% min^{-1}]	W_R [%]
				20%O_2/80%CO_2					
10	288	3.12	418	2.17	-	-	288	3.12	36.38
20	281	6.08	417	4.46	-	-	281	6.08	35.37
40	287	10.25	425	7.52	-	-	287	10.25	36.70
				40%O_2/60%CO_2					
10	275	3.89	375	1.97	-	-	275	3.89	33.89
20	263	11.41	384	4.41	-	-	262	11.41	37.21
40	262	17.47	370	11.41	-	-	263	17.47	36.26
				60%O_2/40%CO_2					
10	252	5.20	-	-	-	-	252	5.20	36.33
20	249	19.35	334	4.15	-	-	249	19.35	34.76
40	247	24.80	338	20.21	-	-	247	24.80	36.54
				80%O_2/20%CO_2					
10	255	35.31	-	-	-	-	255	35.31	35.76
20	251	40.13	-	-	-	-	251	40.13	35.70
40	245	44.66	-	-	-	-	245	44.66	35.21

[1] T_1, T_2, T_3—temperatures corresponding to the first, second, and third peaks of the DTG curve, respectively; D_1, D_2, D_3—rate of mass loss at characteristic points, %/min; D_{max}—maximum rate of mass loss, %/min; T_{max}—temperature at which the maximum rate of mass loss occurs, °C; W_R—mass fraction of the residue after combustion, %.

4. Conclusions

This study investigated the combustion kinetics of municipal sewage sludge in varied O_2/CO_2 atmospheres, with a focus on understanding the effects of different oxygen concentrations on the combustion process. Studies were conducted in different gaseous atmospheres consisting of varying proportions of oxygen and carbon dioxide. The participation of oxygen was 20, 40, 60, 80 and 100% vol. The experimental temperatures varied in the range of 873–1273 K. The following key results were obtained during this study:

- The oxygen concentration in the O_2/CO_2 mixture had a significant impact on the combustion behavior of sewage sludge. Higher oxygen concentrations accelerated the oxidation process, leading to higher reaction rates and greater mass loss at lower temperatures. This highlights the crucial role of oxygen diffusion in determining the overall combustion kinetics.
- The kinetic parameters, including the activation energy (E_a) and pre-exponential factor (K_o), were determined for two different particle sizes. Smaller particles (1 mm) exhibited higher activation energies, suggesting that their combustion is primarily governed by a kinetic mechanism. In contrast, larger particles (2 mm) showed lower activation energies, indicating that oxygen diffusion plays a more dominant role in their combustion.
- While the heating rate influenced the release of volatiles during the initial stages of combustion, it had a limited effect on the oxidation of char. This indicates that char oxidation is primarily diffusion-controlled and the oxygen concentration is a more critical factor than the heating rate in determining the overall reaction rates during this stage.
- The thermogravimetric analysis (TGA) results demonstrated that the combustion process follows a well-defined pattern with distinct stages of moisture evaporation, volatile release and char oxidation. The presence of CO_2 in the combustion atmosphere slightly modify the decomposition behavior by promoting the gasification of carbon residues, which influenced the overall reaction kinetics.

The findings of this study provide interesting insights into the combustion behavior of sewage sludge, particularly under oxy-fuel conditions, which are relevant for waste-to-energy systems and carbon capture technologies. However, further investigation is needed

to scale up the findings to industrial applications, where factors such as the heat transfer, residence time and real-world combustion conditions could influence the kinetics of sludge combustion. Combining combustion with other thermal processes, such as gasification or pyrolysis, could enhance the energy recovery potential and reduce the emissions from sewage sludge treatment.

Author Contributions: Conceptualization, J.B.; methodology, J.B.; software, J.B.; validation, J.B. and B.B.; formal analysis, J.B. and B.B.; investigation, J.B.; resources, J.B.; data curation, B.B.; writing—original draft preparation, J.B.; writing—review and editing, B.B.; visualization, B.B.; supervision, J.B. All authors have read and agreed to the published version of the manuscript.

Funding: This research was funded by the statute subvention of Czestochowa University of Technology, Faculty of Infrastructure and Environment.

Data Availability Statement: Data are contained within the article.

Conflicts of Interest: The authors declare no conflicts of interest. The funders had no role in the design of the study; in the collection, analyses, or interpretation of data; in the writing of the manuscript, or in the decision to publish the results.

References

1. Alonso, J.M.; Abreu, A.H.M.; Andreoli, C.V.; Teixera, P.C.; Polidoro, J.C.; dos Santos Leles, P.S. Chemical characteristics and valuation of sewage sludge from four different wastewater treatment plants. *Environ. Monit. Assess.* **2023**, *196*, 34. [CrossRef] [PubMed]
2. Tao, J.; Wu, S.; Sun, L.; Tan, X.; Yu, S.; Zhang, Z. Composition of Waste Sludge from Municipal Wastewater Treatment Plant. *Procedia Environ. Sci.* **2012**, *12*, 964–971. [CrossRef]
3. Canziani, R.; Spinosa, L. *Sludge from Wastewater Treatment Plants, Industrial and Municipal Sludge*; Butterworth-Heinemann: Oxford, UK, 2019; pp. 3–30.
4. Nascimento, A.L.; Souza, A.J.; Oliveira, F.C.; Coscione, A.R.; Viana, D.G.; Regitano, J.B. Chemical attributes of sewage sludges: Relationships to sources and treatments, and implications for sludge usage in agriculture. *J. Clean. Prod.* **2020**, *258*, 120746. [CrossRef]
5. Lee, H.S.; Bae, S.K. Combustion kinetics of sewage sludge and combustible wastes. *J. Mater. Cycles Waste Manag.* **2009**, *11*, 203–207. [CrossRef]
6. Wen, C.; Lu, J.; Lin, X.; Ying, Y.; Ma, Y.; Yu, H.; Yu, W.; Huang, Q.; Li, X.; Yan, J. Thermal Behavior Prediction of Sludge Co-Combustion with Coal: Curve Extraction and Artificial Neural Networks. *Processes* **2023**, *11*, 2275. [CrossRef]
7. Soria-Verdugo, A.; Garcia-Hernando, N.; Garcia-Gutierrez, L.M.; Ruiz-Rivas, U. Analysis of biomass and sewage sludge devolatilization using the distributed activation energy model. *Energ. Convers. Manag.* **2003**, *65*, 239–244. [CrossRef]
8. Biagini, E.; Lippi, F.; Petarca, L.; Tognotti, L. Devolatilization rate of biomasses and coal–biomass blends: An experimental investigation. *Fuel* **2002**, *81*, 1041–1050. [CrossRef]
9. Werther, J.; Ogada, T.; Borodulya, V.A.; Dikalenko, V.I. Devolatilisation and combustion kinetic parameters of wet sewage sludge in a bubbling fluidised bed furnace. In *The Institute of Energy's 2nd International Conference on Combustion and Emission Control*; Pergamon: London, UK, 1995; pp. 149–158.
10. Ross, I.B.; Davidson, J.F. Combustion of carbon particles in a fluidized bed. *Trans. Chem. Eng.* **1982**, *60*, 108–114.
11. Basu, P.; Ritchie, C.; Halder, P.K. Burning rate of carbon in circulating fluidized beds. In Proceedings of the First International Conference on Circulating Fluidized Beds, Halifax, NS, Canada, 18–20 November 1985; pp. 229–237.
12. Rajan, R.R.; Wen, C.Y. A comprehensive model for fluidized bed coal combustor. *AIChE J.* **1980**, *26*, 642–665. [CrossRef]
13. Liu, M.; Mostaghimi, P. Numerical simulation of fluid-fluid-solid reactions in porous media. *Int. J. Heat. Mass. Transf.* **2018**, *120*, 194–201. [CrossRef]
14. Sohn, H.Y. General approach to fluid-solid reaction analysis and modelling. In *Fluid-Solid Reactions*, 2nd ed.; Elsevier: Amsterdam, The Netherlands, 2020.
15. Sohn, H.Y. Review of fluid-solid reaction analysis—Part 3: Complex fluid-solid reactions. *Can. J. Chem. Eng.* **2019**, *97*, 2326–2332. [CrossRef]
16. Barneto, A.G.; Carmona, J.A.; Alfonso, J.E.M.; Blanco, J.D. Kinetic models based in biomass components for the combustion and pyrolysis of sewage sludge and its compost. *J. Anal. Appl. Pyrolysis* **2009**, *86*, 108–114. [CrossRef]
17. Folgueras, M.B.; Alonso, M.; Diaz, R.M. Influence of sewage sludge treatment on pyrolysis and combustion of dry sludge. *Energy* **2013**, *55*, 426–435. [CrossRef]
18. Chen, X.; Jeyaseelan, S. Study of sewage sludge pyrolysis mechanism and mathematical modelling. *J. Environ. Eng.* **2001**, *127*, 585–593. [CrossRef]
19. Hayhurst, A.N. The kinetics of the pyrolysis or devolatillisation of sewage sludge and other solid fuels. *Combust. Flame* **2013**, *160*, 138–144. [CrossRef]

20. Conesa, J.A.; Marcilla, A.; Prats, D.; Rodriguez-Pastor, M. Kinetic study of the pyrolysis of sewage sludge. *Waste Manag. Res.* **1997**, *15*, 293–305. [CrossRef]
21. Liu, Y.; Liu, Y.; Wang, S.; Chen, T.; Gao, B.; Gao, H.; Wang, H. Independent parallel pyrolysis kinetics of model components in sewage sludge analyzed by BPM neural network. *Environ. Sci. Pollut. Res.* **2023**, *30*, 97486–97497. [CrossRef]
22. Liu, T.; Lang, Q.; Xia, Y.; Chen, Z.; Li, D.; Ma, J.; Gai, C.; Liu, Z. Combination of hydrothermal carbonization and oxy-fuel combustion process for sewage sludge treatment: Combustion characteristics and kinetics analysis. *Fuel* **2019**, *242*, 265–276. [CrossRef]
23. Aidabulov, M.; Zhakupov, D.; Zhunussova, K.; Temireyeva, A.; Shah, D.; Sarbassov, Y. Thermal Characterization, Kinetic Analysis and Co-Combustion of Sewage Sludge Coupled with High Ash Ekibastuz Coal. *Energies* **2023**, *16*, 6634. [CrossRef]
24. Hernandez, A.B.; Okonta, F.; Freeman, N. Thermal decomposition of sewage sludge under N_2, CO_2 and air: Gas characterization and kinetics analysis. *J. Environ. Manag.* **2017**, *196*, 560–568. [CrossRef]
25. Vyazovkin, S.; Burnham, A.K.; Criado, J.M.; Perez-Maqueda, L.A.; Popescu, C.; Sbirrazzuoli, N. Kinetics Committee recommendations for performing kinetic computations on thermal analysis data. *Thermochim. Acta* **2011**, *520*, 1–19. [CrossRef]
26. Galwey, A.K.; Brown, M.E. Isothernal kinetic analysis of solid-state reactions using plots of rate against derivative function of the rate equation. *Thermochim. Acta* **1995**, *267/270*, 1–25. [CrossRef]
27. Sorensen, L.; Saastamoinen, J.; Hustad, J. Evaluation of char reactivity data by different shrinking-core models. *Fuel* **1996**, *75*, 1294–1300. [CrossRef]
28. Liu, K.; Ma, C.Q.; Xiao, H.M. Experimental and kinetic modelling of oxygen-enriched air combustion of paper mill sludge. *Waste Manag.* **2010**, *30*, 1206–1211. [CrossRef]
29. Ciao, H.; Ma, X.; Liu, K. Co-combustion kinetics of sewage sludge with coal and coal gangud under different atmospheres. *Energy Convers. Manag.* **2010**, *51*, 1976–1980.
30. Hu, Y.Q.; Nikzat, H.; Nawata, M.; Kobayashi, N.; Hasatani, M. The characteristics of coal-char oxidation under high partial pressure of oxygen. *Fuel* **2001**, *80*, 2111–2116. [CrossRef]
31. Chen, C.; Lu, Z.; Ma, X.; Long, J.; Peng, Y.; Hu, L. Oxy-fuel combustion characteristics and kinetics of microalgae Chlorella vulgaris by thermogravimetric analysis. *Bioresour. Technol.* **2013**, *144*, 563–571. [CrossRef]
32. Zhou, Z.; Hu, X.; You, Z.; Wang, Z.; Zhou, J.; Cen, K. Oxy-fuel combustion characteristics and kinetic parameters of lignite coal from thermogravimetric data. *Thermochima Acta* **2013**, *553*, 54–59. [CrossRef]
33. Lai, Z.; Ma, X.; Tang, Y.; Lin, H. A study on municipal solid waste MSW combustion in N_2/O_2 and CO_2/O_2 atmosphere from the perspective of TGA. *Energy* **2011**, *36*, 819–824. [CrossRef]
34. Yi, B.; Zhang, L.; Mao, Z.; Huang, F.; Zheng, C. Effect of the particle size on combustion characteristics of pulverized coal in an O_2/CO_2 atmosphere. *Fuel Process Technol.* **2014**, *128*, 17–27. [CrossRef]

Disclaimer/Publisher's Note: The statements, opinions and data contained in all publications are solely those of the individual author(s) and contributor(s) and not of MDPI and/or the editor(s). MDPI and/or the editor(s) disclaim responsibility for any injury to people or property resulting from any ideas, methods, instructions or products referred to in the content.